Thermochimica Acta, 174 (1991) 153–167
Elsevier Science Publishers B.V., Amsterdam

THERMOANALYTICAL OBSERVATIONS ON SYNTHESIS OF OXIDE SUPERCONDUCTORS

M. KAMIMOTO

Electrotechnical Laboratory, Tsukuba, Ibaraki 305 (Japan)

(Received 26 February 1990; in final form 19 June 1990)

ABSTRACT

This paper reviews applications of thermal analysis to the study of the synthesis of high-temperature oxide superconductors. TG and TG–DTA have been most widely used to determine heat treatment conditions for all types of oxide superconductors. Kinetic analysis has been applied successfully and reaction mechanisms have been determined for several synthetic routes of $Ba_2RCu_3O_{7-x}$ ($R \equiv$ rare earth elements).

INTRODUCTION

Since the first oxide superconductor was discovered by Sleight and coworkers [1], research into superconductivity in oxides has been promoted and various oxide superconductors have been synthesized. This has occurred particularly in the last few years after Tanaka and colleagues [2] reconfirmed discovery of the oxide superconductor with the highest critical temperature by Bednorz and Müller [3]. Extensive work has been carried out, being further stimulated by the discovery of the oxide superconductor $Ba_2YCu_3O_{7-x}$ having a critical temperature above liquid nitrogen temperature [4]. Bi–Sr–Ca–Cu [5] and Tl–Ba–Ca–Cu [6] oxide superconductors having higher critical temperatures, and novel materials in which electrons are doped as a carrier [7] have been found recently.

The versatile applicability of thermal analysis was revealed in the research, and many techniques have been applied [8–10]. Measurements of electric resistivity and magnetic susceptibility with temperature change are, in essence, thermoanalytical techniques, i.e., thermoelectrometry (TE) and thermomagnetometry (TM). Observation of non-stoichiometry [8,11] and determination of oxygen content [8] by thermogravimetry (TG) are among the most important applications, because the oxygen content is closely related to superconductivity. The isotope effect on the critical temperature was observed by utilizing oxygen nonstoichiometry. Differential scanning calorimetry (DSC) is applicable: if a superconductor with a critical tempera-

0040-6031/91/$03.50 © 1991 – Elsevier Science Publishers B.V.

TABLE 1

Application of thermal analysis to research into oxide superconductors

Application fields	Techniques [a]
Formation process (+ kinetics)	TG, DTA, EGA, MO, ETA
Crystalline transition	DTA, TD
Melting and glass formation	DTA, MO
Oxygen content	TG (TPR), EGA
Nonstoichiometry	TG, EGA, (TD)
Sintering and crack formation	TD
Thin film formation (expansion matching)	TD
Critical temperature (T_c)	TE, TM, DSC?
Crystal growth (phase diagram)	DTA
Vapor pressure (MOCVD)	TG, EGA, EGD

[a] MO, microscopic observation; ETA, emanation thermal analysis; TD, thermodilatometry; TPR, temperature programmed reduction; TE, thermoelectrometry; TM, thermomagnetometry

ture above the low temperature limit of DSC is found, bulk superconductivity will be confirmed calorimetrically by DSC. Vapor pressure measurement by TG and evolved gas analysis or detection (EGA or EGD) is also important in the development of thin film technology, especially for molecular organic chemical vapor deposition. These applications are summarized in Table 1 [10].

For the synthesis of superconductors, various routes have been used to obtain fine powders, bulk materials, and films of high quality, as shown in Fig. 1. Thermoanalytical techniques, such as TG and EGA, are very useful for observing those synthetic reactions accompanied by gas evolution and mass change. Differential thermal analysis (DTA) can also be applied to the

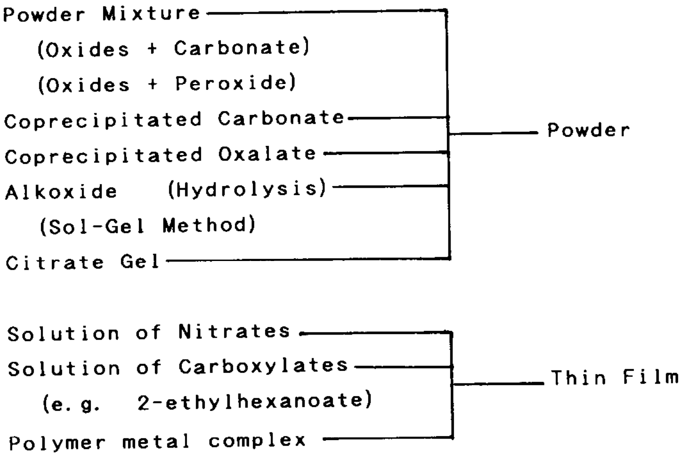

Fig. 1. Various routes for oxide superconductor synthesis.

observation of melting, glass formation and crystallization as well as of synthetic reactions. Thermoanalytical techniques provide us with useful information for synthesis and fabrication.

Thermoanalytic studies on synthesis have been carried out for the following purposes.

(1) To determine temperature conditions of synthesis for:
(i) various routes of synthesis
(ii) different compositions
(iii) different groups of superconductors
(iv) various atmospheres.

(2) To clarify the relation between the characteristics of the synthesized superconductors and the starting materials.

(3) To clarify the mechanisms of the synthesis.

Such information is very important for producing oxide superconductors of good quality.

In order to determine the conditions of the thermal treatment after sintering, thermal analysis of oxygen desorption/absorption played an important role. Annealing at around 400 ° C, to obtain sufficient oxygen, gives superconductors having high critical temperatures. This has been reported by Gallagher and co-workers [8,12] and by Ozawa et al. [11]. The present review focusses on the applications of thermal analysis to synthesis before annealing at around 400 ° C.

THERMAL ANALYSIS OF SYNTHESIS OF $Ba_2RCu_3O_{7-x}$ BY SOLID STATE REACTION OF A MIXTURE OF $BaCO_3$, R_2O_3 (R ≡ RARE EARTH ELEMENTS), AND CuO

A variety of thermoanalytical investigations have been carried out concerning the synthesis of oxide superconductors. Most of the investigations are of $Ba_2RCu_3O_{7-x}$ (R ≡ rare earth elements), since these are the first compounds discovered having critical temperatures higher than liquid nitrogen temperature. Among the many synthesis routes mentioned above, synthesis from a powder mixture of $BaCO_3$, R_2O_3, and CuO has been most widely used.

According to numerous TG–DTA data reported for this process [13–23], the following general features appear in the TG–DTA curves, as shown in Fig. 2.

(1) Mass loss which begins to occur gradually at around 750 ° C, and reaches an almost constant level at temperatures as high as 950 ° C.

(2) An endothermic peak at 810 ° C.

(3) An endothermic peak above 935–975 ° C.

The mass loss is mostly due to CO_2 evolution from $BaCO_3$ during perovskite formation, and partly due to oxygen loss from the superconductor synthesized at higher temperatures. For this perovskite formation pro-

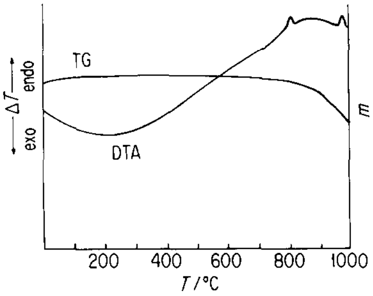

Fig. 2. TG–DTA curve for the thermal decomposition of a mixture of $BaCO_3$, Y_2O_3, and CuO.

cess, TG was applied at various heating rates in order to estimate the necessary duration of the heat treatment. The endothermic peak at 810 ° C is due to a transition of unreacted $BaCO_3$. Superconductors having an unreacted portion of $BaCO_3$ sometimes show a small peak at the same temperature [11]. This endothermic peak thus could be used to evaluate the quality of the synthesized sample, as an alternative to IR spectroscopy. The endothermic peak in a higher temperature region is recognized as a partial melting, although the temperatures reported [13–18] are not always in good agreement with each other. The discrepancy seems to be due to differences in the quality of the samples, and partly due to differences in experimental conditions such as heating rate, atmosphere, and sample mass.

From TG results, Sugai et al. [19] obtained the mass loss of the mixture as a function of sintering time at various temperatures. It was pointed out that sintering below 930 ° C for several hours is insufficient for the complete decomposition of $BaCO_3$ in the mixture.

Brnicevic et al. [20] applied isothermal TG to the investigation of the required heat treatment conditions for obtaining superconductors of high quality. TG of the 1 : 2 : 3 mixture was carried out in air for various sintering conditions. Complete decomposition of $BaCO_3$ was confirmed from the mass loss of the mixture for three-step sintering conditions: 18 h at 860 ° C, 16 h at 900 ° C, and 16 h at 950 ° C. However, under two-step sintering conditions, such as 19 h at 900 ° C and 16 h at 950 ° C, or one-step sintering conditions, 900 ° C for as long as 72 h, a single phase superconductor was not produced. The IR absorption peak of the residual CO_3^{2-} was also observed in the region of 1400 cm^{-1}.

It was also observed [20] that one-step sintering at 950 ° C for 20 h in an oxygen atmosphere gave a superconductor having a T_c of 91 K (the transition region is within 2 K), although it contains a trace of Y_2BaCuO_5.

Paz-Pujalt et al. [21] obtained the XRD patterns for calcination of the mixture at successive temperatures of 600, 700, 800, and 900 ° C. The lines for yttrium oxide, barium carbonate and copper oxide became sharper at 700 ° C. Following thermal treatment at 800 ° C, lines for $BaCuO_2$ together

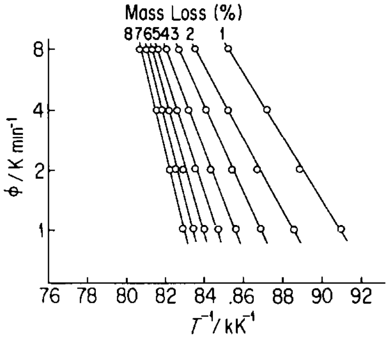

Fig. 3. Heating rate (logarithmic scale) vs. reciprocal absolute temperature at different percentages of mass loss for a mixture of $BaCO_3$, Y_2O_3, and CuO.

with those for $Ba_2YCu_3O_{7-x}$ appeared. Only after prolonged heating at 900 °C, did the XRD pattern show the presence of a single phase 123-perovskite.

Although the heat treatment temperatures are different, the experimental results mentioned above show that calcination of the 1 : 2 : 3 mixture is recommended before final sintering.

According to mass loss vs. time curves, Sugai et al. [19] pointed out that the reaction process obeys a parabolic law on the whole, suggesting interdiffusion between particles of $BaCO_3$, CuO and/or Y_2O_3 as the rate-determining process.

The authors of ref. 22 tried to apply the so-called Ozawa plot to the analysis of TG data at various heating rates in order to estimate the reaction time and to investigate the mechanism of the perovskite formation process. In the Ozawa plot, the logarithm of the heating rate is plotted against reciprocal absolute temperature at a given mass loss, and the activation energies are estimated from the slope of the straight lines. For the mixture, however, the slope changed with mass loss, as shown in Fig. 3. This means that perovskite formation proceeds by many different processes, probably due to the inhomogeneous distribution of the component materials and to the rather large particle sizes in the mixture.

It must be noted that two-component reactions could take place together with three-component perovskite formation in a similar temperature range. Homogeneity and particle size of the starting materials are therefore important to obtain good superconductors.

Gadalla and Hegg [23] investigated the reaction by TG at constant heating rates of 3, 5 and 10 °C min^{-1}. Six overlapping steps occurred during the formation: the first three steps produced the intermediate phases of $BaCuO_2$ and BaY_2CuO_5, while the last three steps were reversible and corresponded to reactions with partial melting. By applying the Coats and Redfern [24] and the Šatava and Skvara [25] techniques to the mass loss, Gadalla and Hegg [23] concluded that the mechanisms for all six processes are diffusion controlled. Their analyses seem to contain some ambiguity, since overlapping between the parallel processes is quite large, as shown in Fig. 4 of ref. 23. Furthermore, each process should start at $\alpha = 0$ and proceed to $\alpha = 1$, where α is the conversion for each process. It is not clear whether this condition was satisfied or not in their analyses.

Kaisersberger et al. [26] applied rate controlled sintering in which the temperature rise was programmed in the quasi-isothermal or stepwise isothermal mode in order to maintain the linear shrinkage at the desired rate. This procedure leads to a 50% higher linear shrinkage for the same material, providing higher mechanical strength and chemical stability of the sintered body. They also investigated the synthesis of $EuBa_2Cu_3O_{7-x}$ by TG.

Schonherr [27] performed a TG study in order to examine the effect of the atmosphere during sintering on the reaction rate for synthesis of $Ba_2YCu_3O_{7-x}$. In a pure oxygen environment the reaction rate was slowed down considerably at the same heating rate.

DTA and TG studies were carried out by Noël and Parent [18] in order to investigate the synthesis and sintering behavior of $Ba_2RCu_3O_{7-x}$ ($R \equiv Y$, Gd or Nd). A proportional relationship was observed between the ionic radius of the rare earth element and the onset of the melting temperature in an oxygen atmosphere: 1030 °C, 1075 °C, and 1107 °C for $Ba_2YCu_3O_{7-x}$, $Ba_2GdCu_3O_{7-x}$, and $Ba_2NdCu_3O_{7-x}$, respectively. These temperatures shifted to lower temperatures in a nitrogen atmosphere.

SYNTHESIS OF $Ba_2RCu_3O_{7-x}$ USING BaO_2 OR BaO INSTEAD OF $BaCO_3$

Use of BaO_2 instead of $BaCO_3$ as a starting material has also been reported [28–30]. Beruto et al. [29] used TG to obtain the required heat treatment conditions for $Eu_2O_3/4BaO_2/6CuO$ and $Ho_2O_3/4BaO_2/6CuO$. In these cases, a liquid phase is formed by the melting of BaO_2 [30], and the mass loss due to oxygen evolution from BaO_2 starts at 500 °C and 700 °C for the two cases, respectively. The TG curves show a plateau above 900 °C, and further mass loss occurs at higher temperatures. Beruto et al. [29] insisted that the plateau temperature is an optimal heat treatment temperature; that of the europium-based oxide is 20 °C lower than that of the holmium-based oxide.

Šesták et al. [31] observed an increase in reactivity also for a mixture of Y_2O_3, CuO, and BaO instead of $BaCO_3$, owing to the formation of a liquid phase in the temperature range 400–500 °C.

SYNTHESIS OF $Ba_2YCu_3O_{7-x}$ FROM THE COPRECIPITATED OXALATE

The preparation methods are described in detail by Hirano [32] in this special issue, and only applications of thermal analysis are reviewed here.

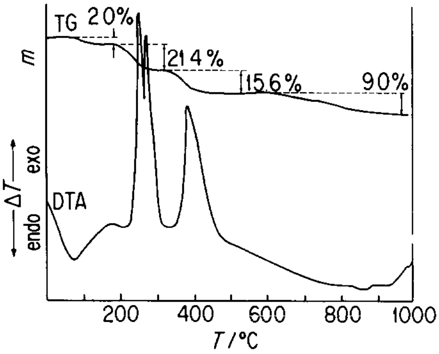

Fig. 4. TG–DTA curve for the thermal decomposition of a coprecipitated oxalate of Ba, Y, and Cu (atomic ratio 2 : 1 : 3).

TG–DTA on the coprecipitated oxalate shows that it first changes to an intermediate product stable below 500 °C (prefired precursor), and then perovskite formation occurs. Figure 4 [11] shows typical results of the TG–DTA study of the thermal decomposition of the coprecipitated oxalate under an oxygen flow.

A small mass loss (2% of the initial sample mass) around 100 °C is presumably due to dehydration. Two stages of decomposition are observed in the temperature ranges 250–320 °C and 380–430 °C. These reactions are thermal decomposition of the oxalate: they are all exothermic reactions owing to combustion of volatilized carbon monoxide to carbon dioxide. From the TG results for the coprecipitated oxalate, Paz-Pujalt et al. [21] concluded that the TG curve was a sum of the individual oxalates, and there was no evidence of an intermetallic oxalate complex.

The X-ray diffraction pattern of the prefired precursor obtained by thermal decomposition at 500 °C changes during a stepwise heating as shown in Fig. 5 [33]. The prefired precursor is characterized by its amorphous structure, consisting of $BaCO_3$ and oxides of yttrium and copper. It was concluded from the X-ray diffraction that the formation of the 123-perovskite starts at 750 °C and is completed at 900 °C; for the coprecipitated oxalate, $BaCuO_2$ was not formed during perovskite formation [21].

The final stage of the mass loss is perovskite formation accompanied by CO_2 evolution from $BaCO_3$. The decomposition of $BaCO_3$ has been confirmed from an EGA study by Negishi et al. [33] and by Paz-Pujalt et al. [21]. Balek and Šesták [34] used emanation thermal analysis (ETA) to investigate synthesis from the coprecipitated oxalate. The ETA curve shows a few peaks reflecting stepwise microstructure changes during heating over a temperature range between 300 °C and 750 °C. ETA thus can be used as a suitable tool for qualitative testing of the intermediate products of oxide superconductors.

A kinetic analysis method [35] was applied to the results of the final stage of thermal decomposition above 750 °C [33]. The activation energies were

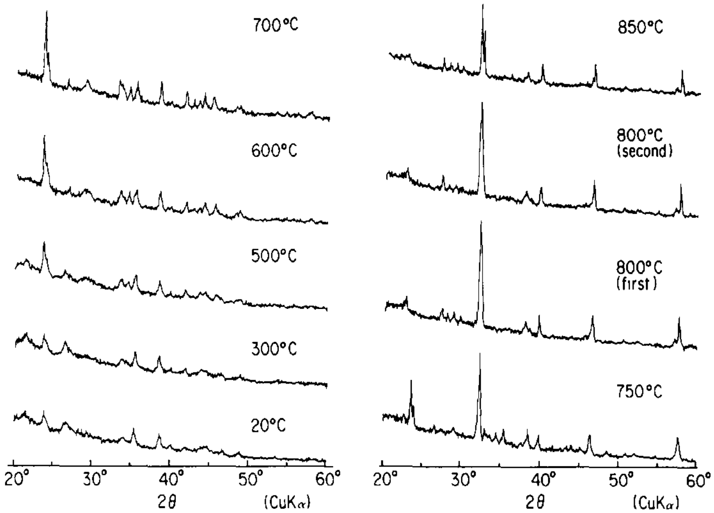

Fig. 5. X-ray diffraction patterns for the prefired coprecipitated oxalate precursor at different temperatures.

estimated from a plot of the logarithm of the heating rate against reciprocal absolute temperature at a given mass loss, resulting in a value of 263 ± 13 kJ mol^{-1}. It is clear that a single elementary reaction takes place in the final thermal decomposition of the precursors made from the coprecipitated oxalate.

By using the activation energy, experimental master curves were obtained (as shown in Fig. 6) for conversion versus generalized time, i.e., the reduced time [33], for each reaction; the master curves can be used to predict the processes under temperature conditions different from those in TG.

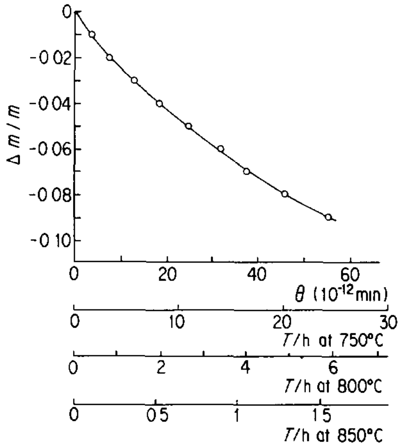

Fig. 6. Mass gain vs. reduced time for perovskite formation from the coprecipitated oxalate.

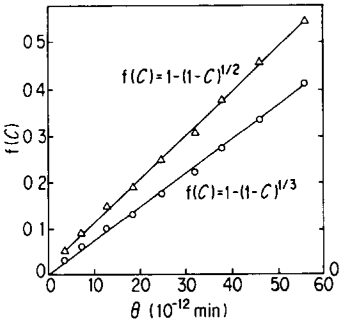

Fig. 7. Plots of $1-(1-C)^{1/2}$ vs. θ and $1-(1-C)^{1/3}$ vs. θ for the coprecipitated oxalate. C is the conversion.

To elucidate the reaction mechanisms, a conventional method for kinetic analysis was applied to the master curves [33]. Surface contracting reactions of both spherical and cylindrical samples were fitted for the decomposition of the prefired precursors from the coprecipitates [33] as shown in Fig. 7. The reaction thus proceeds from the surface to the inside and the rate is proportional to the area of the reacting surface. The reasons for a good fit to the equations for these two mechanisms are assumed to be that the shape of the powder sample is not an ideal sphere but is close to ellipsoid, and that the reaction may proceed in preferential directions of the crystallites.

SYNTHESIS OF $Ba_2YCu_3O_{7-x}$ FROM THE COPRECIPITATED CARBONATE

This preparation method is suitable for obtaining a fine powder. The particles used for the following study [22] had diameters of 0.2-0.3 μm.

The X-ray diffraction pattern of the coprecipitated carbonate fired at 500 °C is similar to the patterns of the coprecipitated oxalate and the mixed 2-ethylhexanoates fired at the same temperature: it contains peaks corresponding to $BaCO_3$ and many diffuse peaks corresponding to oxides of yttrium and copper. Peaks of the perovskite appear at 800 °C together with other peaks; however, heating for 1 h at 800 °C is not sufficient to produce the single compound: after heating for 1 h at 850 °C, only peaks of the perovskite were observed.

TG–DTA was carried out for the prefired precursor which was obtained by maintaining the starting coprecipitate at 500 °C for 1 h. Very similar curves were observed as for other starting materials. Kinetic analysis of the TG data for the final perovskite formation was also carried out. The reaction consists of a single process, and the activation energy was determined to be 282 ± 16 kJ mol^{-1}. For prediction of the reaction time, the actual times for this process occurring at 750, 800 and 850 °C were calculated and are shown in Fig. 8. The reaction mechanism was found to be the

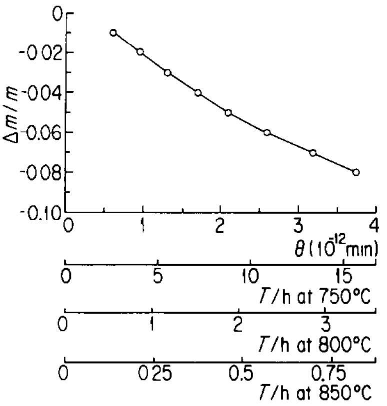

Fig. 8. Mass gain vs. reduced time for perovskite formation from the coprecipitated carbonate.

phase-boundary-controlled contracting interface reaction, as that from the coprecipitated oxalate. The superconductor produced from the finely coprecipitated carbonate powder had a critical temperature onset of 110 K and an end point of 96 K.

SYNTHESIS OF $Ba_2YCu_3O_{7-x}$ FROM METAL CARBOXYLATES

Among several thin film preparation methods, TG has been most extensively applied to synthesis from metal carboxylate precursors [36], particularly mixed solutions of 2-ethylhexanoates of barium, yttrium, and copper. A film with the *c*-axis oriented perpendicular to the film plane has been prepared.

TG–DTA curves of the mixed solutions are merely the sum of the TG–DTA curves of the component solutions [36–38]. The mixed solutions therefore decompose to $BaCO_3$, Y_2O_3, and CuO below 400 °C. The precursor prefired at 500 °C is also in an amorphous state, although crystal growth seems to proceed at lower temperatures compared with precursors from the coprecipitated oxalate and carbonate. Yokota et al. used TG to study decomposition processes of several organic acid salts of barium [39], yttrium [40], and copper [41]. Pyrolysis temperatures of yttrium organic acid salts were found to be dependent on the organic part of the salts as follows: normal chain < cycle < branched chain [40].

It has been pointed out [40] that yttrium oxide formed by the decomposition of yttrium organic acid salts such as 2-ethylhexanoate is amorphous at 400–500 °C and crystallizes at 550 °C. Preparation by the thermal decomposition of naphthanic acid salts [42], metal acetylacetonates [43], and yttrium stearate, barium naphthenate, and copper naphthenate [44] have also been investigated by TG–DTA.

Kinetic analysis of TG data was carried out for a film produced from a solution of the 2-ethylhexanoates [37]. The activation energy for perovskite formation was 269 ± 16 kJ mol^{-1}. A diffusion-controlled reaction of plates was the best-fitting mechanism in this case. The different reaction mechanism seems to arise from differences in the state of the precursors: the 2-ethylhexanoate precursor was made by pyrolyzing a flaky sample several tenths to a few hundred μm in thickness, obtained by evaporating the solvent in a glass dish.

SYNTHESIS OF $Ba_2YCu_3O_{7-x}$ FROM A POLYMER PRECURSOR

Chien and coworkers [45,46] proposed a synthesis by a polymer precursor route. In their method, a polymer–metal complex precursor is first prepared, in which the various metal ions in the desired stoichiometric ratio are homogeneously and uniformly complexed to the polymer. This polymer–metal complex precursor is either cast into a clear film or spun into transparent fibrils. The organic polymer is pyrolyzed, while the metal compounds react to form intermediate intermetallic compounds which are converted in a second reaction in the presence of oxygen.

Other merits of this method are formation at a lower temperature, below 910 °C instead of above 950 °C, shorter fabrication times (1 h), and so on. No thermoanalytical study has been reported so far. Evaluation by thermoanalytical methods will provide further information on this fabrication process.

SYNTHESIS OF Bi–Sr–Ca–Cu–O SUPERCONDUCTORS

Several thermoanalytical investigations have been reported on for the superconductors in this category. They include a melt-quenched process, a sol–gel process, a preparation from metal trifluoroacetate precursors and one from metallo-organic precursors.

Agostinelli et al. [47] applied TG–XRD to the investigation of a metallo-organic decomposition process. The selected precursor molecules were metal carboxylates such as bismuth 2-ethylhexanoate, strontium cyclohexanebutyrate, calcium naphthenate, calcium 2-ethylhexanoate, and copper 2-ethylhexanoate. Mass loss from the mixed carboxylates of Bi, Sr, Ca, and Cu occurs below 200 °C owing to the evolution of solvent followed by the decomposition of precursors and intermediates below 500 °C. After the 550 °C treatment, the films were essentially amorphous according to XRD and consisted of a mixture of oxides and carbonates of metals in the system. At higher temperatures, minor mass losses were observed which include the decomposition of $CaCO_3$ and $SrCO_3$. It was observed that complete decomposition of the carbonates is achieved near 850 ° C, although this is kinetically dependent.

Use of fluoride precursors provides the possibility of improving the superconducting films, since carbon contamination is avoided. Gupta and Cooper [48] used a spin-on solution containing a mixture of Bi, Sr, Ca, and Cu trifluoroacetates as the starting material. TG of the trifluoroacetate mixture (4 : 3 : 3 : 4 composition) in an oxygen atmosphere showed sublimation of the bismuth fluoride. To prevent removal of the bismuth, the decomposition was carried out in moist oxygen. Mass loss and XRD results at different stages showed that the trifluoroacetates are converted to the fluorides, which are then hydrolyzed to the oxides at higher temperatures. In moist oxygen bismuth fluoride was converted to the oxide as soon as it was formed, thus preventing volatilization.

A sol–gel process based on the formation of citrate complexes cannot be used for the Bi–Sr–Ca–Cu–O superconductors since Bi does not form soluble citric acid complexes. Use of ethylene diamine tetra acetic acid (EDTA) makes it possible to keep Bi in solution. Fransaer et al. [49] used TG–DTA to obtain information on the temperatures at which volatile matter is lost from the gel and the temperature at which the decomposition is completed. After the initial loss of water, the 2 : 2 : 1 : 2 oxide exhibited three distinct stages of decomposition. The first major mass loss is mainly due to the break-up of the EDTA compounds into carbonates and nitrates. The final mass loss is the decomposition into the oxide, accompanied by an exothermic DTA peak at 464° C. The mass remains constant even after prolonged heating at temperatures up to the melting point. These facts show that the formation of oxides through the sol–gel process is completed at temperatures far below those in the solid state reactions.

Microscopic observation of the superconductors of this type was made under controlled heating and cooling conditions [50]. The specimen was heated by an IR lamp, and a long-distance objective lens was used for the observation. Partial melting at 815° C and melting at 840 ° C were clearly observed as shown in Fig. 9 (kindly offered by Sinku Riko, Inc.). These temperatures were in good agreement with the peak temperatures of the DTA curve. The microscopic observation thus can be used for characterization of phase changes detected by DTA.

CONCLUDING REMARKS

Applications of thermal analysis to high-temperature oxide superconductors are quite useful for obtaining information on synthetic conditions such as temperatures and treatment time.

As described above, $Ba_2YCu_3O_{7-x}$ is the most suitable substance for kinetic analysis. One reason is that reactions forming $Ba_2YCu_3O_{7-x}$ from

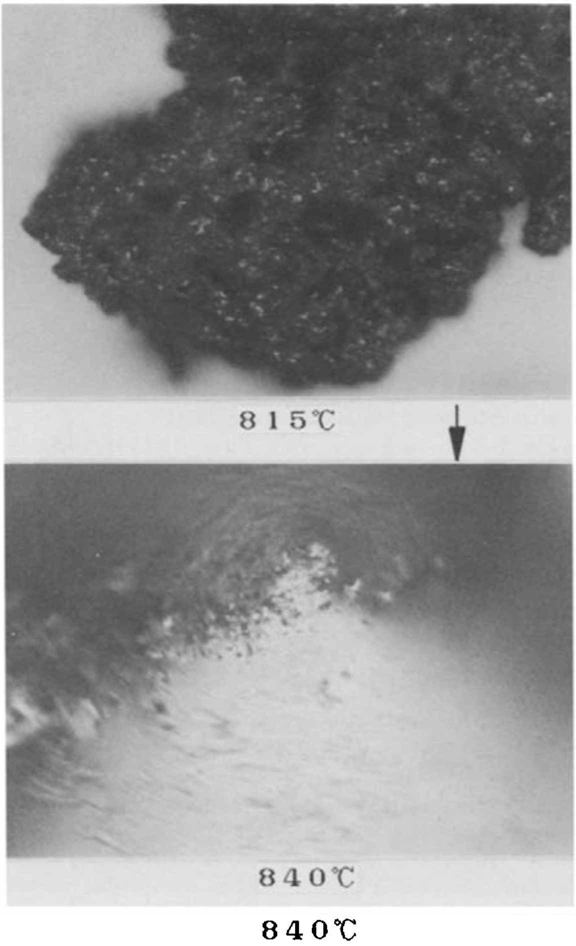

Fig. 9. Microscopic observation (×40) of a mixture of $SrCO_3$, Bi_2O_3, $CaCO_3$, and CuO during heating.

different starting materials can be observed from the beginning to completion using thermal analysis. However, the method described above cannot be applied to the new oxide superconductors, such as the bismuth superconductors, in its original framework. This is because we cannot observe the reactions up to completion using thermal analysis at the usual heating rates due to the low melting temperatures of these compounds. It is also pointed out that bismuth and thallium superconductors are formed by disproportionation of a primary product; for instance, $Bi_2Sr_2CaCu_2O_x$ is formed first and then disproportionation takes place, producing $Bi_2Sr_2Ca_2Cu_3O_x$ and $Bi_2Sr_2CuO_x$ (as shown by electron microscopy [51]). Our TG results also showed that the formation of the Bi–Sr–Ca–Cu–O system from a physical mixture of Bi_2O_3, $SrCO_3$, $CaCO_3$, and CuO consists of parallel reactions.

Some modification in thermal analysis applications is necessary for these cases.

ACKNOWLEDGMENTS

The author would like to thank Dr. Ozawa for his comments on the manuscript of this review.

REFERENCES

1 A.W. Sleight, J.L. Gillson and P.E. Bierstedt, Solid State Commun., 17 (1975) 27.
2 S. Uchida, H. Takagi, S. Tanaka and K. Kitazawa, Jpn. J. Appl. Phys., 26 (1987) L1.
3 J.G. Bednorz and K.A. Müller, Z. Phys. B, 64 (1986) 189.
4 M.K. Wu, J.R. Ashburn, C.J. Torng, P.H. Hor, R.L. Meng, L. Gao, Z.J. Huang, Y.Q. Wang and C.W. Chu, Phys. Rev. Lett., 58 (1987) 908.
5 H. Maeda, Y. Tanaka, M. Fukutomi and T. Asao, Jpn. J. Appl. Phys., 27 (1988) L209.
6 Z.Z. Sheng and A.M. Hermann, Nature, 332 (1988) 55.
7 Y. Tokura, H. Takagi and S. Uchida, Nature 337 (1989) 345; H. Takagi, S. Uchida and Y. Tokura, Phys. Rev. Lett., 62 (1989) 1197.
8 P.K. Gallagher, Adv. Ceram. Mater., 2 (1987) 632.
9 W.P. Brennan, M.P. DiVito, R.F. Culmo and C.J. Williams, Nature, 330 (1987) 89.
10 M. Kamimoto and T. Ozawa, Thermochim. Acta, 148 (1989) 219.
11 T. Ozawa, A. Negishi, Y. Takahashi, R. Sakamoto and H. Ihara, Thermochim. Acta, 124 (1988) 147.
12 P.K. Gallagher, H.M. O'Bryan, S.A. Sunshine and D.W. Murphy, Mater. Res. Bull., 22 (1987) 995.
13 M. Nevriva, E. Pollert, J. Šesták and A. Tříska, Thermochim. Acta, 127 (1988) 395.
14 A. Ono and T. Tanaka, Jpn. J. Appl. Phys., 26 (1987) L825.
15 P. Kishan, L.K. Nagpaul and S.N. Chatterjee, Solid State Commun., 65 (1988) 1019.
16 M. Kikuchi, Y. Shono, A. Tokiwa, K. Oh-ishi, H. Arai, K. Hiraga, N. Kobayashi, T. Sasaoka and Y. Muto, Jpn. J. Appl. Phys., 26 (1987) L1066.
17 R. Sakamoto and M. Kamimoto, unpublished data.
18 D. Noël and L. Parent, Thermochim. Acta, 147 (1989) 109.
19 T. Sugai, G. Oya and S. Imai, Jpn. J. Appl. Phys., 28 (1989) 341.
20 N. Brnicevic, M. Pajevic, Z. Ruzic-Toros, M. Tonkovic, A. Kashta, M. Prester and E. Babic, Solid State Commun., 66 (1988) 633.
21 R.G. Paz-Pujalt, A.K. Mehrotra, S.A. Ferranti and J.A. Agostinelli, Solid State Ionics, 32/33 (1988) 1179.
22 M. Kamimoto, R. Sakamoto, A. Negishi, Y. Takahashi and M. Hirabayashi, Thermochim. Acta, 142 (1989) 281.
23 A.M. Gadalla and T. Hegg, Thermochim. Acta, 145 (1989) 149.
24 A.W. Coats and J.P. Redfern, Nature, 201 (1964) 68.
25 V. Šatava and R. Skvara, J. Am. Ceram. Soc., 52 (1969) 591.
26 E. Kaisersberger, J. Janoschek and W. Hadrich, Thermochim. Acta, 133 (1988) 43.
27 E. Schonherr, Mater. Res. Bull., 23 (1988) 1211.
28 J. Amador, M.T. Casais, C. Cascales and I. Rasines, 9th Int. Congr. on Thermal Analysis, Jerusalem, 23 August 1988, Extended Abstr.

29 D. Beruto, R. Botter, M. Giordani, G.A. Costa, M. Ferretti and G.L. Olcese, Thermochim. Acta, 133 (1988) 27.

30 G.A. Costa, M. Ferretti, E.A. Franceschi and G.L. Olcese, Thermochim. Acta, 133 (1988) 17.

31 J. Šesták, T. Hanslik, M. Nevřiva, D. Zemanova, E. Pollert, A. Tříska and J. Tlaskal, J. Therm. Anal., 33 (1988) 947.

32 S. Hirano, Thermochim. Acta, 174 (1991) 169.

33 A. Negishi, Y. Takahashi, R. Sakamoto, M. Kamimoto and T. Ozawa, Thermochim. Acta, 132 (1988) 15.

34 V. Balek and J. Šesták, Thermochim. Acta, 133 (1988) 23.

35 T. Ozawa, Bull. Chem. Soc. Jpn., 38 (1965) 1881; J. Therm. Anal., 2 (1970) 301; J. Therm. Anal., 9 (1976) 369.

36 T. Kumagai, W. Kondo, H. Yokota, H. Minamiue and S. Mizuta, Chem. Lett., (1988) 551.

37 A. Negishi, Y. Takahashi, R. Sakamoto, T. Ozawa and M. Kamimoto, Thermochim. Acta, 140 (1989) 41.

38 M.E. Gross, P.K. Gallagher and W.L. Brown, Proc. Int. Symp. on Reactivity of Solids, Princeton, 19–24 June 1988.

39 H. Yokota, T. Kumagai and S. Mizuta, Netsu Sokutei, 15 (1988) 97.

40 H. Yokota, T. Kumagai and S. Mizuta, Netsu Sokutei, 15 (1988) 59.

41 H. Yokota, T. Kumagai and S. Mizuta, Netsu Sokutei, 15 (1988) 158.

42 T. Maruyama and T. Nishikawa, Jpn. J. Appl. Phys., 27 (1988) L1693.

43 T. Kumagai, W. Kondo, H. Yokota, H. Minamiue and S. Mizuta, Chem. Lett., (1988) 551.

44 T. Kumagai, H. Yokota, K. Kawaguchi, W. Kondo and S. Mizuta, Nippon Seramikkusu Kyokai Gakujutsu Ronbunshi, 96 (1988) 355.

45 J.C.W. Chien, B.M. Gong, J.M. Madsen and R.B. Hillock, Phys. Rev. B, 38 (1988) 11853.

46 J.C.W. Chien, Polym. Bull., 21 (1989) 1.

47 J.A. Agostinelli, G.R. Paz-Pujalt and A.K. Mehrotra, Physica C, 156 (1988) 208.

48 A. Gupta and E.I. Cooper, Physica C, 158 (1988) 225.

49 J. Fransaer, J.R. Roos, L. Delaey, O. van der Biest, O. Arkens and J.P. Celis, J. Appl. Phys., 65 (1989) 3277.

50 K. Takahashi, personal communication.

51 A. Reller, 9th Int. Congr. on Thermal Analysis, Jerusalem, 23 August 1988, Extended Abstr.